

PROCEEDINGS OF SPIE

SPIDigitalLibrary.org/conference-proceedings-of-spie

Upconversion processes and laser action in $K_5Nd(MoO_4)_4$ stoichiometric crystal

Fernandez, Joaquin, Balda, Rolindes, Iparraguirre, Ignacio, Sanz, Mikel, Voda, M., et al.

Joaquin R. Fernandez, Rolindes Balda, Ignacio Iparraguirre, Mikel Sanz, M. Voda, M. Al-Saleh, Guillermo Lobera, "Upconversion processes and laser action in $K_5Nd(MoO_4)_4$ stoichiometric crystal," Proc. SPIE 4282, Rare-Earth-Doped Materials and Devices V, (27 April 2001); doi: 10.1117/12.424787

SPIE.

Event: Symposium on Integrated Optics, 2001, San Jose, CA, United States

Upconversion processes and laser action in $K_5Nd(MoO_4)_4$ stoichiometric crystal

J. Fernández^{*a,b}, R. Balda^{a,b}, I. Iparraguirre^a, M. Sanz^a, M. Voda^a, M. Al-Saleh^a and G. Lobera^a

^aDept. Física Aplicada I and ^bCentro Mixto CSIC-UPV/EHU, Escuela Superior de Ingenieros, Alameda Urquijo s/n, 48013 Bilbao, Spain

ABSTRACT

In this work we report the upconversion processes that produce blue, green, orange, and red emissions in $K_5Nd(MoO_4)_4$ stoichiometric crystal together with the dynamics and spectral properties of the laser emission. It was found that upconversion energy transfer processes reduce the energy storage capacity through the reduction of the fluorescence lifetimes of the metastable $^4F_{3/2}$ level. The experiments were conducted in such a way that the dynamics of the infrared and visible fluorescence was performed under lasing and nonlasing conditions. The dynamics of the upconverted emission shows that both upconversion energy transfer and excited state absorption of the laser emission occur.

Keywords: upconversion, energy transfer, laser materials, solid state lasers

1. INTRODUCTION

Recently, much attention has been paid to laser materials which are able to combine a high concentration of active ions together with a small light emission quenching. The combination of high concentration and small quenching allows miniaturization of the laser which is interesting for applications in integrated optics. Among oxide laser crystals with a disordered structure, palmierite-type $K_5R(MoO_4)_4$ ($R = Bi, Y, RE = \text{rare earth}$) compounds have generated a great deal of interest as potential stoichiometric laser materials [1]. The crystal structure of $K_5Bi(MoO_4)_4$ [2] was found to be isomorphous with the structure type of palmierite $K_2Pb(SO_4)_2$. These compounds crystallize in the trigonal system, class $\bar{3}m$, space group $R\bar{3}m$. The solid solutions $K_5Bi_{1-x}(RE)_x(MoO_4)_4$ with a small rare-earth concentration present the same palmierite-type structure which is characterized by double layers of $(MoO_4)_4$ tetrahedra perpendicular to the c -axis bonded by $\{K^+\}$ ions arranged between the layers. The remaining K^+ and $(RE)^{3+}$ (or Bi^{3+}) ions, according to their contribution $[K_{0.5}(RE, Bi)_{0.5}]$, are randomly distributed on a plane hexagonal network, embedded within the $(MoO_4)_4$ double layers. On the other hand, the stoichiometric $K_5Nd(MoO_4)_4$ crystal was postulated to be monoclinic. In this case, there are four types of neodymium polyhedra. In two of them, neodymium ions are surrounded by six oxygens whereas for the other two, rare-earth ions occupy centers of symmetry having eight oxygen atoms in their environment [3]. Therefore we should expect two broad crystal field site distributions for neodymium ions in this crystal.

Laser action in this material was reported by Kaminskii et al. by pumping with a Xe-flash tube or a benzene Raman laser [1] and by Lenth et al. by pumping with an argon laser [4]. The use of high power diode lasers as excitation sources has renewed the interest in the spectroscopic and laser properties of solid-state Nd lasers. The intense pumping regime achieved with these high power lasers generates non-linear effects in the laser media which may significantly affect the performance

*Corresponding author: e-mail: wupferoj@bi.ehu.es, Phone: 34-94 601 4044, Fax: 34-94 601 4178.

of rare-earth-based solid state lasers. For instance, upconversion processes can be a loss source if originating in the upper laser level. The upconversion fluorescence can be due to energy transfer upconversion (ETU), excited state absorption of pump radiation (ESAPR), and excited state absorption of laser emission (ESALE) (laser emission or fluorescence from the upper laser level). These higher order effects can significantly affect the performance of many rare-earth-doped solid state lasers. Upconversion has been studied in Nd-doped crystals [5,6], showing that energy transfer upconversion from the ${}^4F_{3/2}$ state is the main loss mechanism.

In this work we report the study of upconversion processes that produce blue, green, orange, and red emissions together with the dynamics of the infrared emission and spectral properties of the laser emission in $K_5Nd(MoO_4)_4$ crystal pumped with a pulsed Ti-Sapphire laser. The upconversion energy transfer processes were conducted in such a way that the dynamics of the infrared and visible fluorescence was performed under lasing and nonlasing conditions.

2. EXPERIMENTAL TECHNIQUES

Solid solutions of the $K_5Bi_{1-x}(Nd)_x(MoO_4)_4$ were formed within the $K_2O-Bi_2O_3-(RE)_2O_3-MoO_3$ system and high optical quality single crystals were grown in our laboratory by the Czochralski technique in the whole concentration range. All crystals were grown under ambient atmosphere in a platinum crucible by pulling them perpendicularly to the c-direction. The Nd^{3+} concentration of the stoichiometric crystal is $2.37 \times 10^{21} \text{ cm}^{-3}$.

The sample temperature was varied between 4.2 and 300 K in a continuous flow cryostat. The room temperature absorption spectra in the 300-2500 nm spectral range were recorded by using a Cary 5 spectrophotometer. The steady-state emission and excitation measurements were made by using a Ti-Sapphire ring laser (0.4 cm^{-1} linewidth) in the 780-920 nm range. The fluorescence was analyzed with a 0.22 m SPEX monochromator, and the signal was detected by a Hamamatsu R928 photomultiplier and finally amplified by a standard lock-in technique.

Lifetime measurements were performed by exciting the samples with a Ti-Sapphire laser, pumped by a pulsed frequency doubled Nd:YAG laser (9 ns pulse width), and detecting the emission with a Hamamatsu R928 photomultiplier. Data were processed by a boxcar integrator.

3. RESULTS AND DISCUSSION

3.1 IR-to-VIS upconversion

Visible upconversion has been observed at room temperature and low temperature in $K_5Nd(MoO_4)_4$ (KNM) crystal under continuous wave (cw) and pulsed infrared (IR) laser excitation, under lasing and non lasing conditions. In this section we are going to present the results under non lasing conditions. The steady-state emission and excitation spectra were obtained by exciting the samples in the 780-920 nm spectral range by using a cw Ti-Sapphire ring laser (0.4 cm^{-1} linewidth). Cut-off filters were used to remove both the pumping radiation and the infrared luminescence from the samples. Under cw excitation in resonance with the ${}^4I_{9/2} \rightarrow {}^4F_{3/2,5/2}$ transitions there is emission in the 500-750 nm region. The spectra show three main bands centered at around 535, 599, and 668 nm. No emission was observed at wavelengths shorter than 500 nm. However under pulsed excitation in resonance with the ${}^4I_{9/2} \rightarrow {}^4F_{3/2}$ transition, in addition to the three visible bands we also observe a weak blue fluorescence around 389 nm, 420 nm, and 452 nm. As an example Fig. 1 shows the polarized time-resolved emission spectra at 77 K obtained by exciting at 867 nm in resonance with the ${}^4I_{9/2} \rightarrow {}^4F_{3/2}$ transition and at $1 \mu\text{s}$ after the laser pulse. The inset inside the figure shows the blue luminescence.

To identify each upconverted emission band, we have used the low temperature emission spectra given in Fig. 1 and the energy level diagram of Nd^{3+} in KNM crystal shown in Fig. 2. The three main bands observed in the emission spectra have been reported in other Nd-doped materials, and attributed to transitions from the ${}^4G_{7/2}$ level [6-8]. An analysis of the energy level diagram and the upconverted emission spectra suggests that these bands can be attributed to radiative transitions ${}^4G_{7/2} \rightarrow {}^4I_{9/2}$ (535 nm), ${}^4G_{7/2} \rightarrow {}^4I_{11/2}$ (599 nm) and ${}^4G_{7/2} \rightarrow {}^4I_{13/2}$ (668 nm). The dependence of the three lines intensity on the pump power is nearly quadratic which indicates a two photon upconversion process. The observed weak blue emission corresponds to levels with higher energies (${}^4D_{5/2}$, ${}^4D_{3/2}$ or ${}^2P_{3/2}$) than those reached by two infrared photons (see the energy level diagram in Fig. 2).

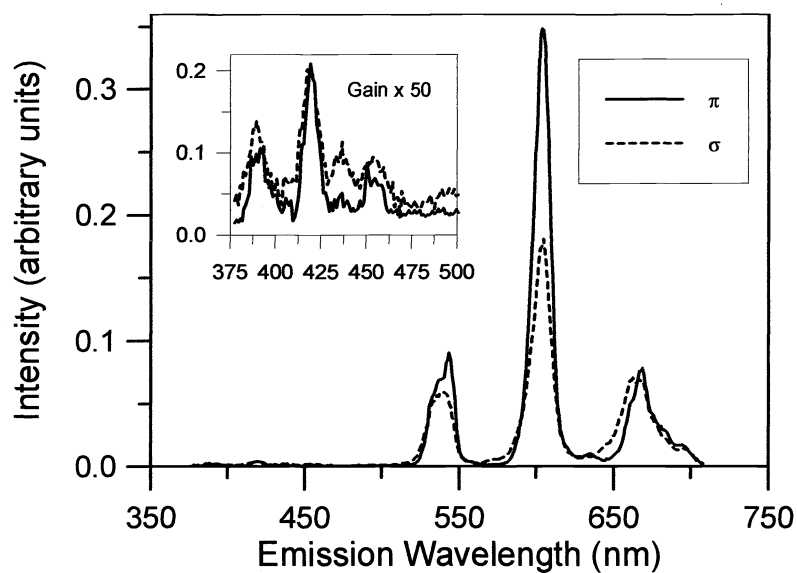


Figure 1. Polarized upconverted emission spectra obtained by exciting at 867 nm at 1 μ s after the laser pulse. Data correspond to 77 K.

The excitation spectra of the visible emissions were investigated in the 780-920 nm range (by using the Ti-Sapphire tunability). Similar excitation spectra were obtained by collecting the luminescence at 535, 599, and 668 nm. As an example, the excitation spectrum of the upconverted emission at 599 nm is presented in Fig. 3 together with the excitation spectrum recorded for infrared emission at 1064 nm for comparison. As can be observed the excitation spectrum shows similar peaks corresponding to the $^4I_{9/2} \rightarrow ^4F_{3/2}$ transition, with no significant differences with the one-photon excitation spectrum.

Together with the energy level diagram of Nd^{3+} ion in KNM, Fig. 2 illustrates the possible mechanisms of population losses from the $^4F_{3/2}$ doublet leading to upconversion processes: excited state absorption (ESA) and/or energy-transfer upconversion (ETU) by pumping either the $^4F_{3/2}$ or $^4F_{5/2}$ manifolds. Concerning the first process, by pumping in the $^4F_{3/2}$ state there is not a good energy matching between the $^4F_{3/2}$ state and $^2P_{1/2}$ level by means of an additional IR photon, and therefore we expect a very low probability for such a process. However, if the excitation is made in the $^4F_{5/2}$ level, a second IR photon could allow an upward transition to the $^2D_{5/2}$ multiplet. The second mechanism (ETU) occurs via dipole-dipole interaction of two excited Nd^{3+} ions in the $^4F_{3/2}$ state. In this case, when two Nd^{3+} ions are excited to the $^4F_{3/2}$ state, a transfer occurs by which one ion loses energy and goes to the 4I_J ($J=11/2, 13/2$) states while the other one gains energy and goes to the $^2G_{9/2}$ or $^4G_{7/2}$ state. These processes can coexist, contributing to the excitation into higher levels. As can be observed the excitation spectrum shows the peaks corresponding to the $^4I_{9/2} \rightarrow ^4F_{3/2}$ absorption band, with no significant differences with the absorption spectrum, which indicates that resonant absorption of the pump radiation is not produced from the metastable $^4F_{3/2}$ state. This behavior suggests that an ETU process seems to be more likely for the observed visible luminescence from the $^4G_{7/2}$ state. Referring to the blue and UV bands, the most probable origin of the upconverted fluorescence seems to be the $^4D_{3/2}$, $^2P_{3/2}$ levels, though the level reached by upconversion could be $^4D_{5/2}$, $^4D_{1/2}$ or even higher levels. These levels can be populated by excited state absorption of laser emission. In this process, Nd^{3+} ions in the $^4G_{7/2}$ state can be excited to the $^4D_{5/2}$ or $^2P_{3/2}$ multiplet by absorbing photons from 1.06 μ m or 1.3 μ m laser emission or fluorescence.

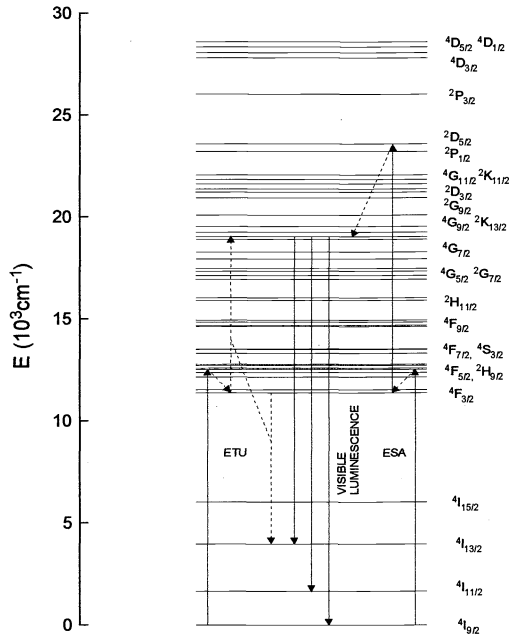


Figure 2. Energy levels of Nd^{3+} in KNM crystal obtained from the low temperature (11 K) absorption spectrum.

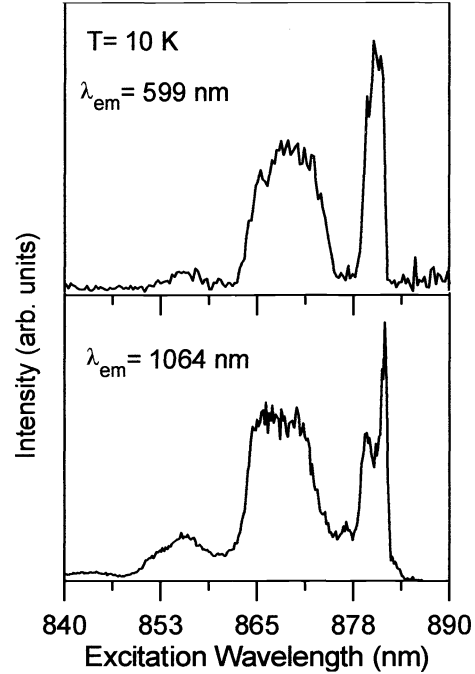


Figure 3. Excitation spectra of the Stokes and anti-Stokes fluorescence from the levels ${}^4\text{F}_{3/2}$ and ${}^4\text{G}_{7/2}$.

The ETU upconversion processes can reduce the population of the upper laser level or cause its lifetime shortening. As a consequence, there is an increase of the laser threshold and a reduction of the energy storage efficiency. These upconversion mechanisms have been studied in Nd-doped glasses [9] and crystals [5-8], showing that energy transfer upconversion from the ${}^4\text{F}_{3/2}$ state is the main loss mechanism. In our case we have evaluated this effect for KNM crystal. The excited state population decay of the ${}^4\text{F}_{3/2}$ state, assuming that the Nd excited states are uniformly distributed throughout the lattice, can be expressed by:

$$\frac{dN}{dt} = -\frac{N}{\tau} - 2W_{ETU}N^2 \quad (1)$$

Where N is the population density, τ is the fluorescence lifetime in absence of upconversion and W_{ETU} is the macroscopic ETU parameter. With $N(t=0)=N_0$, integration yields [10]:

$$N(t) = \frac{N_0 \exp\left(-\frac{t}{\tau}\right)}{1 + 2 W_{ETU} N_0 \tau \left[1 - \exp\left(-\frac{t}{\tau}\right)\right]} \quad (2)$$

So, when there is no upconversion, the decay is purely exponential, whereas for $W_{ETU} \neq 0$, as $W_{ETU}N_0\tau$ increases, the decay time is shortened.

The temporal evolution of the upconverted emissions and the infrared emission of the ${}^4\text{F}_{3/2} \rightarrow {}^4\text{I}_{9/2}$ transition was obtained by exciting the samples at 867 nm in resonance with the ${}^4\text{F}_{3/2}$ level with a Ti-Sapphire laser pumped by a doubled pulsed Nd :YAG laser. As expected, at low excitation power, the decay curves for the ${}^4\text{F}_{3/2}$ state are nearly single exponentials;

however at higher excitation powers an increasing nonexponentiality appears. The results are plotted in Fig. 4 which shows the decay curves at low ($N_0 = 2 \times 10^{17} \text{ cm}^{-3}$) and high excitation power ($N_0 = 2 \times 10^{19} \text{ cm}^{-3}$). As can be seen, a fast nonexponential section is observed at the beginning of the decay, followed by a slower exponential decay which approaches the intrinsic decay time. N_0 is calculated by knowing the pulse energy absorbed, the excited volume of the sample, and the pump photon energy. For the nonexponential decays an average lifetime was calculated by using

$\langle \tau \rangle = \frac{\int I(t) dt}{I(0)}$, where $I(t)$ is the fluorescence intensity. The average lifetime is also related to the population of the ${}^4F_{3/2}$ state

by $\langle \tau \rangle = \frac{\int N(t) dt}{N(0)}$. Using the expression (2), we can obtain :

$$\langle \tau \rangle = \frac{\text{Ln}(1 + 2\tau W_{ETU} N_0)}{2W_{ETU} N_0} \quad (4)$$

Thus the lifetime decrease depends only on the product $W_{ETU} N_0 \tau$. This equation can be used to obtain W_{ETU} , as N_0 is known from the pump intensity, τ from the weak excitation decay, and $\langle \tau \rangle$ from integrating the area under the fluorescence decay at the higher excitation level. W_{ETU} is the only unknown parameter in eq. (4). The reduction in lifetime versus the initial excited population of the ${}^4F_{3/2}$ state is shown in Fig. 5 at two different temperatures 77 K, and 295 K. The theoretical curves give a good fit to the experimental data with an upconversion rate $W_{ETU} = (1.9 \pm 0.06) \times 10^{-16} \text{ cm}^3 \text{ s}^{-1}$ ($T = 77 \text{ K}$) and $W_{ETU} = (2.5 \pm 0.1) \times 10^{-16} \text{ cm}^3 \text{ s}^{-1}$ ($T = 295 \text{ K}$).

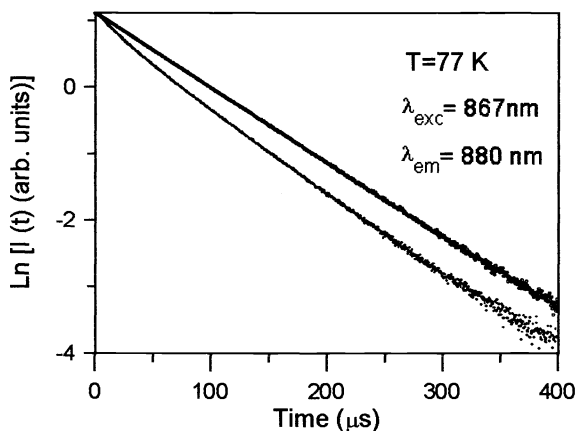


Figure 4. Decay of the IR fluorescence from the ${}^4F_{3/2}$ state for weak excitation, upper curve, and high excitation, lower curve.

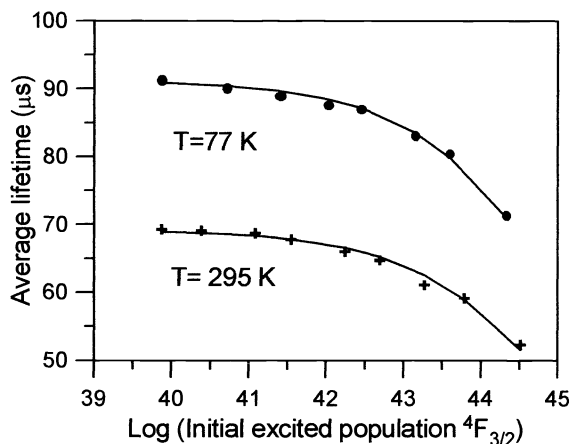


Figure 5.- Variation of the average lifetimes with the initial ${}^4F_{3/2}$ population, and the fit (solid lines) to eq. (4).

We have also obtained the macroscopic ETU parameter by fitting the experimental decay curves of the ${}^4F_{3/2}$ state to Eq. (2). The fluorescence lifetime used in this equation was obtained from the low excitation power experiments. The obtained W_{ETU} value was $1.92 \times 10^{-16} \text{ cm}^3 \text{ s}^{-1}$ ($T = 77 \text{ K}$) and $2.3 \times 10^{-16} \text{ cm}^3 \text{ s}^{-1}$ ($T = 295 \text{ K}$) and the loss inducing parameter $\tau W_{ETU} = 1.8 \times 10^{-20} \text{ cm}^3$ at 77 K and $1.6 \times 10^{-20} \text{ cm}^3$ at 295 K.

The temporal evolution of the upconverted emissions was obtained by exciting the samples in resonance with the ${}^4F_{3/2}$ state. The experimental decays of the main visible bands, which are not single exponentials, present a rapid initial decay followed by a longer nonexponential decay. Similar temporal evolutions are observed for the green, orange, and red emissions. As an example, the logarithmic plot of the experimental decays of the 599 nm and 420 nm emissions at 295 K is shown in Fig. 6. The long term part of the decay curves of the upconverted VIS lines (green, orange, and red) is much longer ($\approx 15 \mu\text{s}$) than

that of the ${}^4G_{7/2}$ state under direct excitation (the lifetime values of the ${}^4G_{7/2}$ and ${}^4G_{5/2}$ level obtained under direct excitation which are too short to be measured with our equipment, have been measured to be less than 10 ns in fluoride crystals [8]). This behaviour suggests that we are dealing with a typical ETU process [8]. The decays of the upconverted blue emissions also show a long term component about 5 μ s but in this case if we assume, as indicated in Fig. 2, that these emissions come from levels ${}^4D_{3/2}$, ${}^2P_{3/2}$, it is not possible to assign them unambiguously to an ETU process due to the metastable character of level ${}^2P_{3/2}$.

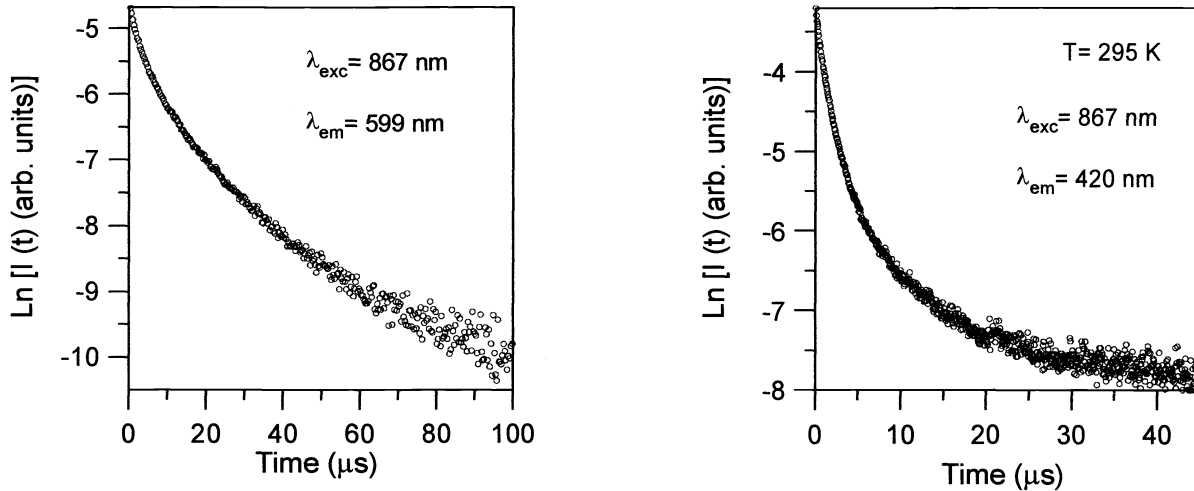


Figure 6. Experimental decay curves of the upconverted fluorescence.

3.2 Laser experiments

For the laser experiments a c-cut crystal plate of dimensions $2 \times 8 \times 20 \text{ mm}^3$ was used. The pump source was a tunable pulsed Ti-sapphire laser (10 ns pulse width and about 30 mJ energy). The pump pulse entered the sample perpendicularly to the center of the $2 \times 8 \text{ mm}^2$ face which was Brewster angle cut to allow transversal pumping. The resonator was a 15 cm long symmetric confocal one, with both high reflectivity coated mirrors. The threshold energy was 12 mJ, and the time-width of the laser output pulse, measured by using a photodiode of 2 ns rise time, was about 100 ns.

Spectroscopic measurements of the laser output as a function of the laser pulse polarization show that the spectral width of the laser spectrum is almost twice for π than for σ polarization. Moreover, the spectral behavior for π polarization shows two main peaks about 1065 nm and 1067 nm which could be related with the presence of two main distributions of crystal field sites for the rare-earth with a strong spectral overlapping, as shown by the site-selective spectroscopy results [11]. Figure 7 shows the room temperature laser spectra obtained at two different laser polarizations.

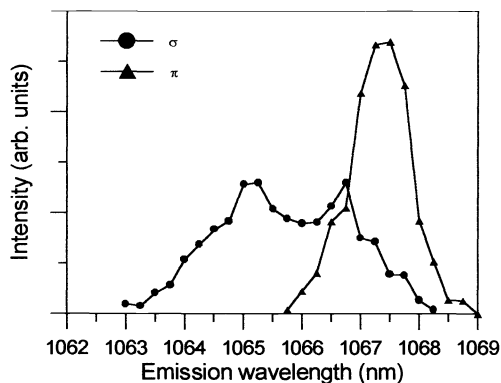


Figure 7. Room temperature stimulated emission spectra of Nd in KNM crystal obtained at two different laser polarizations.

To investigate the influence of the laser emission at 1065 nm on the upconverted fluorescence, we have studied the time evolution of the visible luminescence under lasing conditions. In this case excited state absorption of the laser emission (ESALE) from ${}^4F_{3/2}$ and ${}^4G_{7/2}$ multiplets can play a significant role to populate both ${}^4G_{7/2}$ and ${}^4D_{3/2}$, ${}^2P_{3/2}$ manifolds.

Figure 8 shows the time evolution of the blue and orange emissions (solid lines), under laser action inside the resonator, together with the laser output pulse (symbols). As can be seen during the laser pulse ($\cong 100$ ns), there is a sudden increase of the intensity of the blue and orange upconverted emissions followed by a rapid decrease as the laser pulse disappears. After the laser pulse, the visible emissions present a temporal behavior similar to that found under nonlasing conditions. This behavior suggests that during the laser pulse the populations of the upper states giving the blue and orange fluorescence are strongly enhanced by the laser action. It is worthy to notice that the laser emission is in resonance with the energy difference between ${}^4F_{3/2}$ and ${}^4G_{9/2}$ levels so ESALE can populate the ${}^4G_{9/2}$ level and, from then on, ions in this level can populate the ${}^4G_{7/2}$ multiplet by nonradiative relaxation. Referring to the blue emission the intensity increase during the laser pulse could be explained by ESALE from the ${}^4G_{7/2}$ multiplet which populates the ${}^4D_{5/2}$, ${}^4D_{1/2}$ upper levels. According to the energy level diagram of Nd^{3+} ion in KNM crystal this process is resonant and could be quite efficient.

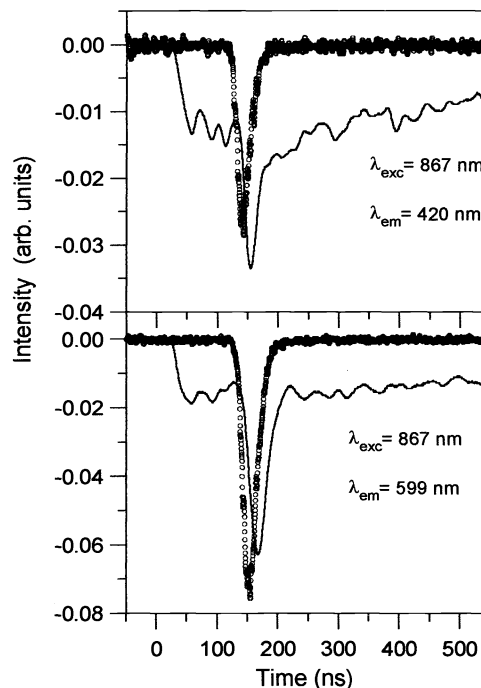


Figure 8. Experimental decay curves of the upconverted emissions and laser output pulse.

5. CONCLUSIONS

The study of upconversion processes in KNM crystal has shown that infrared excitation in levels ${}^4F_{5/2}$ or ${}^4F_{3/2}$ lead to green, orange, and red emissions from the ${}^4G_{7/2}$ level. Under pulsed excitation in the ${}^4F_{3/2}$ multiplet additional blue emissions are also observed. The main upconverted visible bands correspond to green, orange, and red fluorescence from the ${}^4G_{7/2}$ level. The temporal dependence of the decays from these emissions, together with the excitation spectra features suggest that an energy transfer upconversion is the dominant mechanism for the population of level ${}^4G_{7/2}$ in this crystal. Energy transfer upconversion processes involving two Nd ions in the ${}^4F_{3/2}$ cause the lifetime shortening of the upper laser state. From the analysis of lifetime measurements of the ${}^4F_{3/2}$ state at different initial excited populations we have estimated the macroscopic ETU parameter and the loss inducing parameter.

The spectroscopic measurements of the laser output as a function of polarization of the laser pulse show that the spectral width of the laser spectrum is almost twice for π than for σ polarization. Moreover, the spectral behavior for π polarization shows two main peaks around 1065 nm and 1067 nm which could be related with the presence of two main distributions of crystal field sites for the rare-earth with a strong spectral overlapping, as shown by the results of site-selective spectroscopy.

The temporal evolution of the visible emission under lasing conditions shows an intensity increase of the blue and orange emissions during the laser output pulse.

ACKNOWLEDGEMENTS

This work was supported by the Spanish Government CICYT Ref. MAT97-1009, Basque Government (PI97/99), and Basque Country University (G21/98).

REFERENCES

1. A.A. Kaminskii, S.E. Sarkisov, J. Bohm, P. Reiche, D. Schultze, and R. Uecker, "Growth, Spectroscopic and Laser Properties of Crystals in the $K_5Bi_{1-x}Nd_x(MoO_4)_4$ system", *Phys. Stat. Sol. (a)* **43**, pp. 71-79, 1977.
2. P.W. Klevtsov, L.P. Kozeeva, V. I. Protasova, L. Yu. Kharchenko, L. A. Glinskaya, R. F. Klevtsova, and V. V. Bakakin, "Synthesis of crystals and X-ray diffraction investigation of double molybdates $K_5Ln(MoO_4)_4$, $Ln=La-Tb$ ", *Sov. Phys Crystallogr.* **20**, pp. 31-33 (1975).
3. B. I. Lazoryak and V.A. Efremov, "Structure of palmierite-like $K_5Nd(MoO_4)_4$, $K_5Bi(MoO_4)_4$, and $Rb_5Gd(MoO_4)_4$ ", *Sov. Phys. Crystallogr.* **31**, pp. 138-142, 1986.
4. W. Lenth, H.-D. Hattendorff, G. Huber, and F. Lutz, "Quasi-cw Laser Action in $K_5Nd(MoO_4)_4$ ", *App. Phys.* **17**, pp. 367-370, 1978.
5. Y. Guyot, H. Manaa, J.Y. Rivoire, R. Moncorgé, N. Garnier, E. Descroix, M. Bon, and P. Laporte, "Excited-state-absorption and upconversion studies of Nd^{3+} -doped single crystals $Y_3Al_5O_{12}$, $YLiF_4$, and $LaMgAl_{11}O_{19}$ ", *Phys. Rev. B* **51**, pp. 784-799, 1995.
6. T. Chuang and H.R. Verdún, "Energy-transfer up-conversion and excited state absorption of laser radiation in Nd-YLF crystals", *IEEE J. Quantum Electron.* **32**, pp. 79-91, 1996.
7. J.H. Schloss, L.L. Chase and L.K. Smith, "Dynamics of laser-pumped Nd^{3+} laser media at high excitation energy", *J. Lumin.* **48&49**, pp. 857-862, (1991).
8. J.D. Zuegel and W. Seka, "Upconversion and reduced $^4F_{3/2}$ upper-state lifetime in intensely pumped Nd:YLF", *Appl. Optics* **38**, pp. 2714-2723, 1999.
9. S.A. Payne, G.D. Wilke, L.K. Smith, W.F. Krupke, "Auger upconversion losses in Nd-doped laser glasses", *Opt. Commun.* **111**, pp. 263-268, 1994.
10. S. Guy, C.L. Bonner, D.P. Shepherd, D.C. Hanna, A.C. Troper, and B. Ferrand, "High-Inversion Densities in Nd:YAG: Upconversion and Bleaching", *IEEE J. Quantum Electron.* **34**, pp. 900-909, 1998.
11. M. Voda, I. Iparraguirre, J. Fernández, R. Balda, M. Al-Saleh, A. Mendioroz, G. Lobera, M. Cano, M. Sanz, and J. Azkargorta, "Laser properties of Nd^{3+} in $K_5Nd(MoO_4)_4$ stoichiometric disordered crystal", *Optical Materials* (in press)